Mathematical Modelling of Radiobiological Parameters

6

Piernicola Pedicini, Lidia Strigari, Luigi Spiazzi, Alba Fiorentino, Paolo Tini, and Luigi Pirtoli

Introduction

All treatment strategies are studied at the preclinical and clinical level, and the related endpoints are used to extract radiobiological parameters in mathematical models. This chapter aims to provide an overview of these approaches based on clinical and cellular data.

P. Pedicini
I.R.C.C.S. Regional Cancer Hospital C.R.O.B., Rionero-in-Vulture, PZ, Italy

L. Strigari (✉)
Laboratory of medical physics and expert systems, Regina Elena National Cancer Institute, via E. Chianesi 53, Rome 00144, Italy
e-mail: strigari@ifo.it

L. Spiazzi
Physics Department, Spedali Civili Hospital, Brescia, Italy

A. Fiorentino
Sacro Cuore Don Calabria Hospital, Negrar-Verona, Italy

P. Tini
Tuscany Tumor Institute, Florence, Italy

Unit of Radiation Oncology, University Hospital of Siena (Azienda Ospedaliera-Universitaria Senese), Viale Bracci 11, Siena, 53100, Italy

L. Pirtoli
Tuscany Tumor Institute, Florence, Italy

Unit of Radiation Oncology, Department of Medicine, Surgery and Neurosciences, University of Siena, Siena, Italy

As mentioned in the previous chapter, median survival of glioblastoma (GBM) patients is poor. In fact, the 1-year median survival rate of GBM patients is approximately 50 %, despite the use of aggressive standard treatments, i.e. macroscopic resection and radiochemotherapy followed by adjuvant temozolomide.

In particular, to date most patients die from disease progression, primarily local recurrence. In fact, the limited tolerance of normal tissues can lead to inadequate therapeutic radiation doses.

The use of modern treatment planning systems, combined with a multi-imaging modality and the possibility to use Image Guided Radiotherapy (IGRT) images in order to track dose deposits in the tumour, allows a reliable cumulated dose to be delivered to the tumour bed. One of the characteristics of this dose is, in many cases, the lack of homogeneity, due to the proximity of Organs at risk (OAR). Nevertheless, the dose grid dimension (8–12 mm^3 voxel volume) and imaging resolutions limit the dose delivery tracking to a cellular level. The use of inaccurate dosimetric data is one of the main flaws of model parameter estimations obtained from literature on clinical findings from the last decade.

In addition, when deriving model parameters from meta-analysis, the heterogeneity in investigated patient populations can lead to different values or produce contrasting results to those of individual studies. This is known as Simpson's paradox [1].

L. Pirtoli et al. (eds.), *Radiobiology of Glioblastoma*, Current Clinical Pathology,
DOI 10.1007/978-3-319-28305-0_6

The effect of tissue, or cell, irradiation depends on the dose but in general is not proportional (in probability or intensity) to the dose. The inherent stochastic nature of the interaction of radiation–matter, the cellular structure and the complexity of environmental interaction make it difficult to develop a simple and reliable model of cell killing [1–3].

The cumulative effect of dose delivery to tissue makes it impossible to derive the correct dose for each specific patient and cell type, which would maximize the benefit of irradiation in terms of probability of cure, severity of deterministic damage and probability of stochastic side effects [1].

Therefore, the necessity to define an adequate population based pattern of temporal and spatial dose delivery has seen the development of various models of cell killing and tumour control probability (TCP).

The first studies that involved the combined effect of dose per fraction and overall treatment time (OTT) were performed as early as the 30s [4, 5], but they were neglected in consequences of World War II. The first universally accepted model focused on the skin reaction was published in 1944 [6], accompanied by great uncertainty on energy and source to skin distance values limiting its application to modern radiotherapy.

The first model of lethal doses based on radiosensitivity of tumour cells and Poisson statistics was presented in 1961 [7].

In 1969, Ellis suggested a formula which related total dose, number of fractions and OTT to a quantity termed "Nominal Standard Dose". The authors intended, this quantity to represent "the biological effect of a given treatment regime" and enable the comparison of various treatment schedules (with different dose fraction, total dose and overall treatment times) [8]. Considering the poor prognosis for GBM patients in the late 70s, the scientific community paid greater attention to the dose effect for GBM [9] and the first attempts to correlate delivered dose and tissue damage by means of Computer Tomography scans were published [10].

In the past 20 years, an increased number of research projects aiming at simulating and formulating the mechanisms of tumour response to radiation treatment have been proposed. One of most simple and efficacious models for radiation response is the linear-quadratic (LQ) model proposed by Fowler [11, 12]. The LQ model describes cell survival after exposure to ionizing radiation and is expressed by a linear radiobiology parameter α (intrinsic whole tumour radiosensitivity) and a quadratic parameter β (repair capability) with reference to two forms of DNA damage.

The LQ model determines the relative contribution of each selected dose schedule to the surviving fraction. However, it could be optimized by taking into account cell repopulation parameters, such as the kick-off time for tumour repopulation (T_k), the repopulation doubling time (T_d) and the effective tumour repopulation rate quantified by $\gamma = \ln 2/T_d$ [3, 13–21].

Cellular Dose Response Models

Cell Killing

The basic assumption of the simple LQ model states that the surviving cell fraction after a homogeneous dose irradiation is [11]

$$S(D) = e^{-(\alpha D + \beta D^2)} \tag{6.1}$$

where D is the dose and Biological Effective Dose (BED) defined as

$$BED = D\left(1 + \frac{D}{\alpha/\beta}\right) \tag{6.2}$$

When assuming that more than a single fraction is delivered, each with a dose d_i, then (6.1) becomes

$$S(D) = e^{-\left(\alpha \sum_i d_i + \beta \sum_i d_i^2\right)} \tag{6.3}$$

If the dose d is delivered in each fraction then (6.3) becomes

$$S(D) = e^{-n(\alpha d + \beta d^2)} \tag{6.4}$$

and (6.2) becomes

$$BED = nd\left(1 + \frac{d}{\alpha/\beta}\right) \tag{6.5}$$

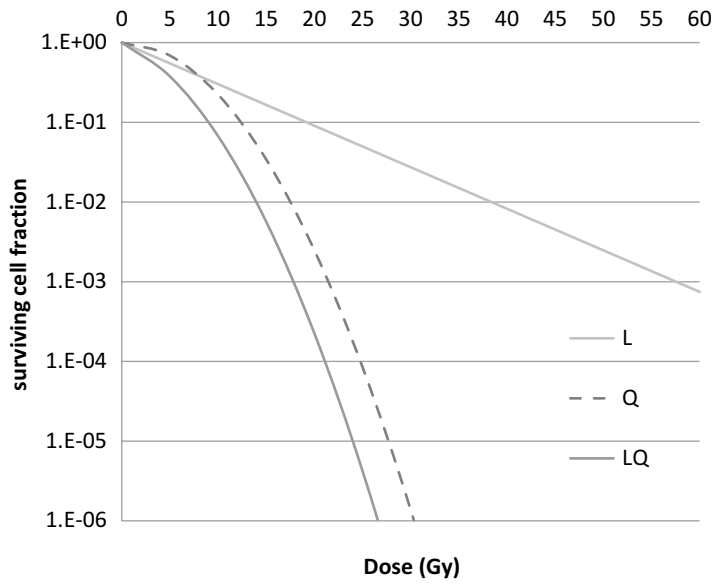

Fig. 6.1 Cell survival against dose due to the linear (L), i.e. αD, and quadratic (Q), i.e. βD^2 component. The combined effect is shown as LQ. The used parameters are $\alpha = 0.12$/Gy and $\alpha/\beta = 8$ Gy

It is easier to describe BED in terms of equivalent dose given at 2 Gy per fraction [14, 22]

$$EQD_2 = D\frac{d+\alpha/\beta}{2Gy+\alpha/\beta} \tag{6.6}$$

A graphical representation of the cell survival curve for the linear and quadratic component is shown in Fig. 6.1. The parameter α corresponds to the initial slope of the cell survival curve (i.e. the larger values of α correspond to the steeper initial slope) while β determines the degree of downward curvature of the cell survival curve (the larger value of β corresponds to the more "bent" curve).

Incomplete Repair

The LQ model as described in (6.1)–(6.6) cannot correctly estimate incomplete repair and OTT [23]. A formula that includes appropriate correction factors that link EQD_2 for a dose given within T days to one given in t is:

$$EQD_{2T} = D_t\frac{d\left(1+H_m\right)+\alpha/\beta}{2Gy+\alpha/\beta} - \left(T-t\right)D_{prolif} \tag{6.7}$$

where H_m is the incomplete repair factor and the suffix m is equal to the fractions per day if it is assumed that there is a complete repair within the following day. D_{prolif} is a parameter that gives the "lost" dose per day of delay. Some authors prefer to use a different symbol, λ [24].

Low-Dose Hypersensitivity

Although the LQ approach is widely used to describe tumour cell killing, at low doses (<1 Gy) the survival fraction does not monotonically decrease like the dose [25, 26]. In the range 10–30 cGy the surviving fraction is constant, while the radioresistance increases, reaching a maximum around 1 Gy and thereafter the curve shows a decreasing slope [25]. These results indicate a counter-intuitive effect, i.e. at low dose the cell surviving fraction increases with dose. Of note, the stated increased dose is not a subsequent irradiation, but a complete different irradiation with a different dose level.

Equation (6.1) can be corrected to take into account this effect [26]

$$S\left(D\right) = e^{-\left(\alpha_s D\left(1+\left(\alpha_s/\alpha_r-1\right)\exp\left[-D/D_C\right]\right)+\beta D^2\right)} \tag{6.8}$$

Genome-Dependent Radiation Sensitivity

Haas-Kogan et al. [27], using LQ and repair-saturation mathematical models, showed that p53 function influences the effect of fractionated radiotherapy on GBM tumours. They identified two distinct cellular responses to radiation, p53-independent apoptosis and p53-dependent G1-arrest, influencing radiobiological parameters that characterize the GBM radiation response. Some years later, a distinct genotype-dependent radiosensitivity group was identified in association with mutant ATM (ataxia telangiectasia mutated), wild-type TP53 (tumour protein 53) and mutant TP53 linked to intrinsic cellular radiosensitivity of GBM cell lines that grouped into four different radiosensitivity categories. This suggests the existence of multiple genotype-dependent mechanisms underlying the intrinsic cellular radiosensitivity [28, 29].

The coexistence of glioma-differentiated cancer cells (GDCC) and glioma-cancer stem cells (GCSCs) has been proposed to explain the intrinsic tumour heterogeneity to radiation response. The GCSCs have been reported to be less sensitive to radiation-induced damage through preferential activation of DNA damage checkpoint responses. Other authors [30, 31] have suggested that GCSCs can readily assume a quiescent state and later, following DNA repair, repopulate the tumour. DNA damage induced by radiotherapy treatment potently initiated activation of phosphorylation of the ATM, p53 and Chk2 checkpoint proteins. Phosphorylation of these checkpoint proteins resulted significantly higher in the GCSCs compared to GDCCs and could explain the reported intrinsic radiosensitivity difference [32, 33]. A model that simulates the coexistence of GCSC and GDCCs and their cell cycle phase in growth and radiation response has recently been proposed [34]. The authors integrated the LQ model, extended to take into account the effects of inter-fraction tumour repopulation and α and β cell-specific radiosensitivity parameters, with the introduction of ξ and λ as radiation protection factors for quiescent cells and GCSCs, respectively. The simulations performed revealed that not only the higher intrinsic radioresistance of GCSCs but also the presence of a shift from asymmetric to symmetric division or a fast cycle of GCSCs after fractionated radiotherapy may contribute to the frequently observed accelerated repopulation after irradiation. The survival and increase of the GCSCs population during radiation therapy may be a leading cause of accelerated and more aggressive GBM recurrence after radiation therapy.

Dual Compartment Tumour Survival, Mathematical Model

In an attempt to model subpopulation GCSCs, dual compartment tumour survival, a mathematical model has recently been proposed by Yu et al. [35]. The model assumes the radiation response as the sum of two subpopulations deriving from the coexistence of GCSCs and GDCCs, each with their distinctive LQ parameters. Thus, the dual compartment cell survival model is constructed as

$$S(D) = f \cdot e^{-\left(\alpha_1 D + \beta_1 D^2\right)} - (1-f) \cdot e^{-\left(\alpha_2 D + \beta_2 D^2\right)} \quad (6.9)$$

where f is the fraction of GCSCs, (1−f) is the fraction of GDCCs, while α_i and β_i describe the radiobiological properties (intrinsic radiosensitivity and repair capacity) of each population. The increased radioresistance has been explained by the rapid regrowth of the GDCC compartment triggered by its depletion while a viable GCSC population is maintained.

Figure 6.2 illustrates the surviving fraction of two populations with $\alpha_1 = 0.12$/Gy (cell line#1), $\alpha_2 = 0.6$/Gy (cell line#2) and of a mixed population 50 % cell line#1 + 50 % cell line#2, with the same α_i/β_i ratio (i.e. 8 Gy).

The type of programmed cell death, as the response to treatment in glioma cells, has been widely debated in recent years, suggesting that cell autophagy is the main intracellular process involved and not apoptosis [36].

A dual compartment cell survival model has been proposed by Tini et al. [37] to explore the cell-autophagy role after in vitro irradiation of

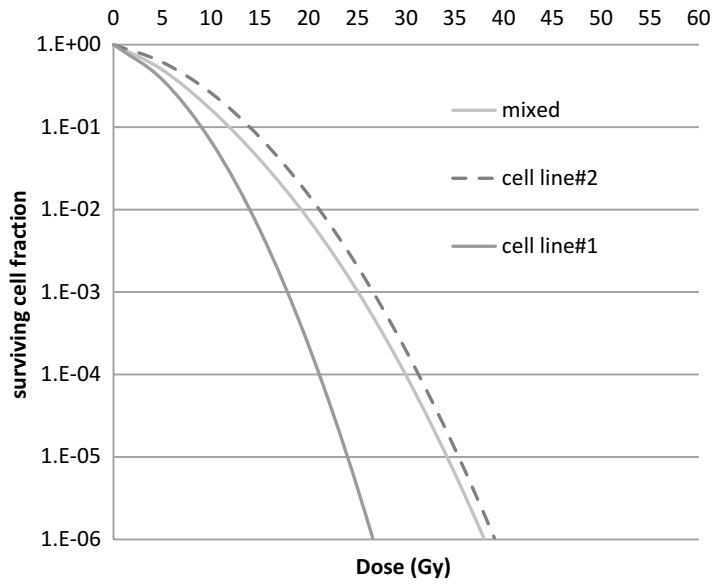

Fig. 6.2 The surviving fraction of two populations with $\alpha_1 = 0.12$/Gy (cell line#1), $\alpha_2 = 0.6$/Gy (cell line#2) and of a mixed population (50 % cell line#1 + 50 % cell line#2), assuming the same α_i/β_i ratio (i.e. 8 Gy)

glioma cells (T98G, U373) integrating the low-dose hypersensitivity effect in its formulation. This model assumes radiation response in glioma cells derived by activation of cell autophagy involved in both the pro-survival mechanisms and direct programmed cell death (i.e. programmed autophagy-related cell death) [38]. This model that fits complex survival curves in T98G and U373 glioma cell lines in the presence of multi-modal response to radiation is formulated as

$$S(D) = A \cdot e^{-(\alpha_s D)} + (1 - A) \cdot e^{-\left[(\alpha_r - \delta)D + \beta D^2\right]} \quad (6.10)$$

where the parameters represent

A = effect of low-dose hypersensitivity

α_s = irreversible pro-death autophagy induced by DNA damage

α_r = not irreversible autophagy pro-death

δ = autophagy pro-survival

β = repairable DNA damage

TCP

Even in the simpler case of homogeneous irradiation the use of Poisson statistics to describe the probability that all clonogenic cells are killed has proven to be incorrect [39], this has led to the development of models based on cellular killing [24, 40–42]. All these models are based, more or less explicitly, on some assumptions [41]:

- Each tumour is made of a cluster of non-interactive clonogenic cells
- Radiosensitivity may vary between tumour (and patients)
- A tumour is controlled if all the clonogenic cells are inactivated
- Clonogenic cell inactivation is a mutually independent event

The combination of these assumptions allows the development of a statistical model based on the probability of inactivation of all clonogenic cells. The number of clonogenic tumour cells is critical in determining the TCP and some authors have based it on the initial tumour volume, as given by the following equation:

$$V = a \cdot N^b \quad (6.11)$$

where a and b are constant. Figure 6.3 illustrates the TCP against the dose when the number of

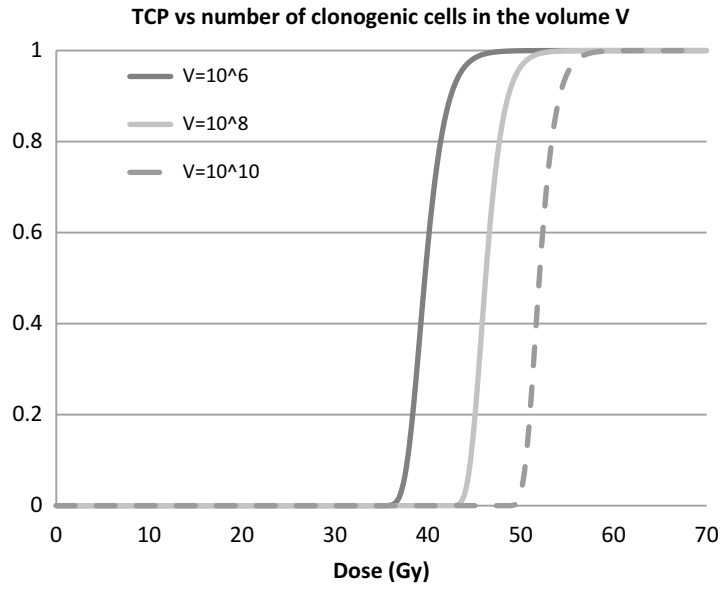

Fig. 6.3 The TCP behaviour against the delivered dose when the number of clonogenic cells in the volume V increases from 10^6 to 10^{10}

clonogenic cells in the volume V increases from 10^6 to 10^{10}.

These formulations are derived by statistical assumption as follows:

$$TCP = \frac{1}{(2\pi)^{\frac{3}{2}}\sigma_{\ln k}\sigma_\alpha\sigma_\lambda}, \int_{+\infty}^{-\infty} e^{-\exp\left(k'-\alpha' D-\beta D^2/N+\lambda' T\right)} e^{\left(k'-\ln(k)\right)^2/\left(2\sigma_{\ln k}^2\right)} e^{(\alpha'-\alpha)^2/\left(2\sigma_\alpha^2\right)} e^{(\lambda'-\lambda)^2/\left(2\sigma_\lambda^2\right)} d\lambda' d\alpha' dk' \quad (6.12a)$$

where the parameters ln(k), α and λ represent the clonogenic number, cellular sensitivity and repopulation rate, respectively [41].

$$TCP = \frac{1}{k}\sum_{K}^{i=1}\prod_{M}^{j=1} e^{-\rho_j V_i f_j \exp\left(-\alpha_i D_i-\beta_i D_i^2\right)} \quad (6.12b)$$

where in the original model [40] the quadratic term βD_i^2 was omitted for simplicity.

In (6.12b), D_i is the dose received by a specific subunit and has to be considered fixed within the subunit, while ρ_j is the variable clonogenic cell densities within the volume, each having a relative volume fraction f_j.

The third model uses a different EQD_2 formulation that considers the surviving fraction

$$S(d) = S(2Gy)^{\frac{d}{2Gy}\left(\frac{\alpha/\beta+d}{\alpha/\beta+2Gy}\right)} \quad (6.12c)$$

The TCP formulation includes radiosensitivity variability intra-patient (ind) and inter-patient (pop), assuming these variations can be described by the variability of S(2 Gy) [41].

$$TCP = \int G_{pop}\left(\overline{S(2Gy)}^{ind}, \overline{S(2Gy)}^{pop}, \sigma^{pop}\right) TCP_{ind}\, d\overline{S(2Gy)}^{ind} \quad (6.13)$$

where

$$TCP_{ind} = e^{-NC\sum_{NP}^{i=1}\left(v_i \overline{S(d_i)}\right)} \quad (6.14)$$

$$\overline{S(d_i)} = \int G_{ind}\left(S(2Gy)^{ind}, \overline{S(2Gy)}^{ind}, \sigma_{ind}\right) S(d_i)\, dS(2Gy)^{ind} \quad (6.15)$$

$$S(d_i) = S(2Gy)^{\sum_{n}^{k=1} \frac{d_k}{2Gy}\left(\frac{\alpha/\beta + d_k}{\alpha/\beta + 2Gy}\right)} \quad (6.16)$$

where NP is the number of dose bins, NC is the number of clonogenic cells, n the number of fractions and ν_i the volume corresponding to the i-th dose point. The probability density functions are expressed as follows [42]:

$$G_{pop}\left(\overline{S(2Gy)}^{ind}, ,\overline{S(2Gy)}^{pop}, ,\sigma^{pop}\right) = \frac{1}{\sqrt{2\pi}\sigma_{pop}} e^{-\left[\frac{\left(\overline{S(2Gy)}^{pop} - \overline{S(2Gy)}^{pop}\right)^2}{2\sigma_{pop}^2}\right]} \quad (6.17)$$

$$G_{ind}\left(S(2Gy)^{ind}, \overline{S(2Gy)}^{ind}, \sigma^{ind}\right) = \frac{1}{\sqrt{2\pi}\sigma_{ind}} e^{-\left[\frac{\left(S(2Gy)^{ind} - \overline{S(2Gy)}^{ind}\right)^2}{2\sigma_{ind}^2}\right]} \quad (6.18)$$

Models described above involve a wide number of parameters with statistical uncertainty. Notwithstanding this, the radiobiological models represent the only possible strategy to optimize treatment, compare rival plans or fractionation schemes or give an estimation of TCP at a given time after therapy.

Unfortunately, a radiobiological model able to overcome the poor GBM response to radiation is currently unavailable, due to the incomplete understanding of the underlying genetic and biomolecular alterations. Profiling studies based on gene or protein expression have revealed several altered, common, molecular pathways, resulting in the subclassification of distinct molecular subtypes (classical, mesenchymal, proneural, neural) that are different in terms of their prognosis and response to therapy [43]. This characterization is not currently in use in clinical practice. Furthermore, emerging evidence shows the existence of a stem like cell compartment in GBM, which demonstrates an increased resistance to ionizing radiation [16, 44, 45]. Due to the higher probability of killing radiosensitive cells with greater efficacy, all tumours during the course of treatment increase the mean radioresistance. GBM is characterized not only by an increase of the mean radioresistance, but also of the maximum.

There are other cellular models based on the possibility of a change in radioresistance during treatment [46] but their complexity is far beyond the aim of this chapter.

Correlating Results of Cell-Culture SF with Clinical Empirical Data at Different Total Doses and Dose Per Fraction

The concept of *isoeffective doses* has been widely investigated in order to link the absorbed dose to the incidence of a specific biological effect attributable to irradiation. Survival curves have been obtained based on in vitro studies, providing some useful information on radiosensitivity of the investigated tumour and normal tissue cells. In particular, the α/β ratio has been derived to measure the sensitivity of the tumour or tissue to fractionation, i.e. to predict how the total dose for a given effect will change when the size of dose fraction is changed.

By using various treatment schedules for in vivo studies, the slope of the isoeffect curves has been determined, highlighting that they change according to the size of dose per fraction and depending on tissue type [47].

Also using in vivo data, the sensitivity to changes in fractionation schedule can be quantified by using the α/β ratio. A high α/β ratio (range, 7–20 Gy), as in acutely responding tissues and in tumours, indicates a more linear survival response of the target cells; a low α/β ratio (range, 0.5–6 Gy), as in late responding tissues, defines a significant curvature in the survival curve of the target cells. As a consequence, the effects of fractionation are rela-

tively greater in the acutely responding than late responding tissues.

This suggests that acute responding tissues have flatter curves than late responding tissues, i.e. fractionation spares the late responding tissues. Of note α/β ratios could be different when calculated using (6.1) or (6.12b), as they are derived from different datasets with different weights to data, corresponding to low and high doses.

Clinical Dose Response Models

Poisson Hypothesis

In the clinical setting, TCP models derived from LQ based on the Poisson hypothesis have been used as a tool to estimate a radiobiological set of parameters from the available clinical outcome [47, 48].

The following equation predicts the progression-free survival based on the Poisson hypothesis

$$PFS = e^{-N\cdot e^{-D(\alpha+\beta d)+\frac{\ln 2}{T_d}(T-T_k)}} \tag{6.19}$$

A graphical method to estimate the radiobiological parameters in (6.19) by using a multiple step procedure has been proposed [48] and shown here in Fig. 6.4.

To combine the clinical outcomes from different published studies, different irradiation schedules need to be used. When comparing two fractionation regimens (e.g. a and b) (6.19) becomes:

$$\frac{\ln\left(PFS_a\right)}{\ln\left(PFS_b\right)} = e^{-N\cdot e^{\alpha(D_b-D_a)+\beta(D_b d_b-D_a D_a)+\frac{\ln 2}{T_d}(T-T_k)}} \tag{6.20}$$

In this formula, the dependence by cell number N and T_k disappeared. Moreover, (6.20) takes into account the different radiotherapy schedules and the related clinical outcome.

Therefore, when a sufficient number of different schedules and a large number of patients are enrolled (to reduce the stochastic fluctuations), an estimation of the cellular parameters (α, β and T_d) can be made by the following equation:

$$\frac{\alpha}{\beta} = \frac{d_b D_b - d_a D_a}{\frac{1}{\alpha}\left[C + \frac{\ln 2}{T_d}\left(T_b - T_a\right)\right] - \left(D_b - D_a\right)} \tag{6.21}$$

where

$$C = \ln\left(\frac{\ln\left(PFS_a\right)}{\ln\left(PFS_b\right)}\right) \tag{6.22}$$

and C is named "clinical efficacy factor".

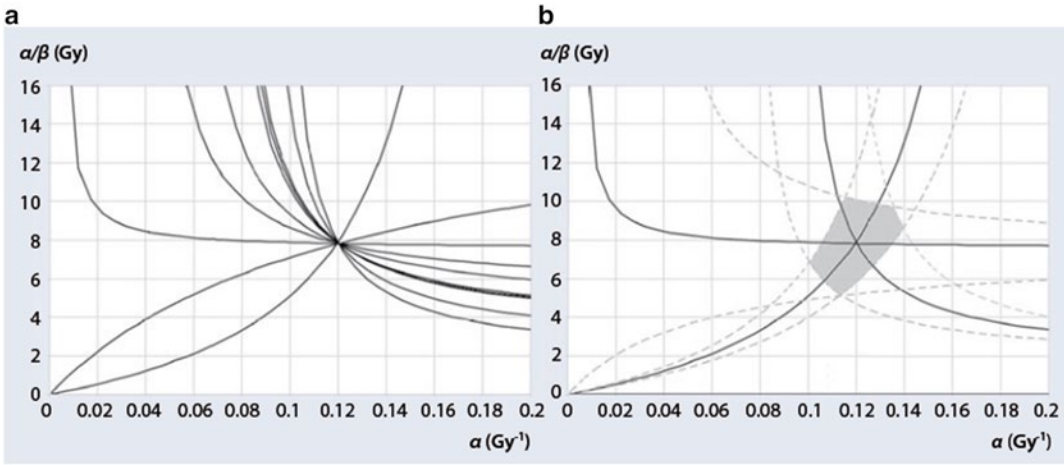

Fig. 6.4 The relationship between α and α/β for glioblastoma multiforme. The black curves have been obtained from (6.19) using couples of clinical data and by varying T_d value up to the coincidence for all curves. The intersections of the curves represent the best estimate of α, α/β and T_d (**a**). The grey curves represent the 95 % confidence interval (only three curves shown) and the shaded area indicates the overall range of uncertainties (**b**)

Equation (6.21) establishes an independent relationship between α and α/β from which it is possible to include and compare studies with different clinical outcomes when $C \neq 0$.

The curves of different schedules are plotted in the α versus α/β graph. T_d is varied until the coincidence of all curves is obtained, thus the intersection point provides an estimate of α, $\alpha/\beta$and T_d. This expedient allows the values of N and T_k and their uncertainties in subsequent steps to be calculated.

Moreover, (6.21) is also substantially independent from the impact of chemotherapy (i.e. temozolomide, TMZ, or bischloroethylnitrosourea, BCNU), which is unknown or indistinguishable when this approach is used, chemotherapy being generally adopted in all the investigated schedules or presenting limited differences in terms of radiosensitivity when different drugs are adopted.

Once the estimate of α, β and T_d is made, an estimation of D_{prolif}, in fraction of 2 Gy, is obtained by the following equation:

$$D_{prolif} = \frac{\ln 2}{T_d \cdot (\alpha + 2\beta)} \tag{6.23}$$

Subsequently, an estimation of T_k is obtained using the hypothesis of stem cells activation by the following equation [49]:

$$T_k = \frac{7 \ln(N_0 / N_A)}{5d(\alpha + \beta d)} \tag{6.24}$$

Assuming that the process of stem cell activation for accelerated proliferation could begin when the tumour population has decreased to the order of a few thousand cells (e.g. $\ln(N_0/N_A)3000$), thus $T_k = \frac{11}{d(\alpha + \beta d)}$ [49].

Table 6.1 Model parameters entracte from Pedicini et al. [47]

Parameter	Best estimate	$CI_{95\,\%}$
α(Gy^{-1})	0.12	0.10–0.14
β (Gy^{-2})	0.015	0.013–0.020
α/β (Gy)	8	5.0–10.8
T_d (days)	15.4	13.2–19.5
D_{prolif} (Gy)	0.3	0.22–0.39
T_k (days)	37	29–46
N (clonogens)	9.1×10^3	4.0×10^3–2.1×10^4

Finally, the estimation of N is performed by using (6.19), in which α, α/β, T_d and T_k are fixed at the best values. All the above steps produce the best fit parameters useful to compare predicted TCP curves and experimental data.

The best estimate and the $CI_{95\%}$ for α, α/β, T_d, N, T_k and D_{prolif} are shown in Table 6.1.

Multivariate Logistic Regression

In order to consider the combined effects (e.g. of drug delivery and radiotherapy approach, as well as patient age, and other variables), a multivariate logistic regression can be adopted to predict the TCP following preoperative CRT. The TCP can be expressed as:

$$P(z) = \frac{e^z}{1 + e^z} \tag{6.25}$$

where

$$z = a_0 + a_1 D + a_2 D \cdot d + a_3 OTT + a_4 \cdot age + a_5 \cdot 5FUdose + a_6 \cdot cisplatindose + a_7 \cdot mitomycinCdose \tag{6.26}$$

In this approach, the LQ dose response model may incorporate not only the total radiotherapy dose and dose per fraction to estimate the α/β ratio [50], but also the other clinical and patient based covariates. Although they have no theoretical biological rationale, they nonetheless provide a useful numerical estimate of the true relationship for the range of values experienced in common practice. This model that in principle is applicable to GBM has so far only been applied to oesophageal cancer.

Time-Dependent TCP

The survival of GBM patients, usually about 50 % at 1 year and decreasing over time, can be modelled [9] as follows including a time factor:

$$S^{\prime\left(D_j,\tau\right)} = e^{-N\cdot e^{-\left[\alpha D+\beta GD^2-\gamma\left(T-T_k\right)\right]e^{-a\tau}}} \quad (6.27)$$

where τ is the time after the treatment completion for the given dose *Dj*.

Here, the authors assumed that the survival rate depends exponentially on relapse time and the parameter a has been estimated using a fitting procedure for survival rate at 0.5, 1.0 and 1.5 years, using clinical data reported by Walker et al. [9] and by Salazar et al. [51, 52].

Finally, in the paper of Qi et colleagues, the α and α/β parameters have been provided for malignant gliomas with grade 3 or 4 [53] .

Model Parameters

The selection of proper LQ parameters has been challenging particularly in the clinical setting for GBM. The repair half time for sublethal damage repair, T, is assumed to be 0.5 h [54].

An interpretation of the radiobiological parameters may help clinicians to identify an optimal fractionation schedule. In particular, an α/β of 8 Gy indicates high fractionation sensitivity while an α of 0.12 Gy^{-1} supports a high intrinsic radiosensitivity of this tumour. Consequently, these parameters correspond to a low β value (0.015 Gy^{-2}), which represents a high capability of GBM cells to repair the radiation damage. Moreover, based on the fit of clinical data, the T_d shows a moderate value (15.4 days), together with a very long T_k (37 days). This implies that the tumour radiation response with the OTT is substantially independent, thereby endorsing hypofractionation (doses greater than 2 Gy/fraction) or hyper-fractionation (doses less than 2 Gy/fraction with multiple daily sessions) schedules. This is supported by the outcome of hypofractionated studies that adopt a treatment of 25 Gy in which the reduction of OTT did not improve overall survival or progression-free survival, PFS (with a 1 PFS of 29.42 %) [55].

From another point of view, a higher value of γ supports a strong dependence on OTT of the results can be explained by the selection of radioresistant stem cells, which are recruited during irradiation and tend to repopulate quickly [49, 56–59].

The best fit curve ($N = 9.1 \times 10^3$) and its confidence interval (6.0×10^3–1.4×10^4) indicate that a limited number of aggressive cells are able to repopulate tumour. Moreover, a long T_k together with a moderate repopulation indicates substantial independence of the therapeutic results from the duration of the OTT. However, this mechanism appears to be negligible when compared to the mechanism of repair, which should be more pronounced in this cell type. This characteristic can be taken into account in favour of the time required by OAR in order to fully repair the radiation damage.

Model parameters indicate a strong dependence on total dose, thus an improvement of clinical results might be obtained with an increase in the total dose rather than with a reduction of the OTT. Based on the estimated radiobiological parameters, an increase of the total dose up to a BED of approximately 92 Gy (total dose, 74.8 Gy; dose per fraction, 2.2 Gy; 34 fractions) should lead to a TCP greater than 0.85. This result appears to be surprisingly higher than that obtained with standard fractionation (60 Gy × 30 fractions with a BED of approximately 74 Gy), which is approximately 0.3. This optimistic prediction by the model still requires mandatory confirmation. The fitted curve has $\gamma 50 = 3.31$, which is very close to the mean $\gamma 50$ of the clinically relevant range ($\gamma 50 = 3.20$) described in the literature [25, 60].

Parallelism Between Classical and Biomolecular Modelling in Glioblastoma

Rockne and other authors included the effects of radiation therapy using the LQ radiobiological model in a tri-dimensional proliferation and infiltration (PI) model [61–65]. The PI model was developed in the early 1990s by Tracqui et al. [66] to describe the diffuse PI of glioma cells in

the human brain. In this model, the rate of change of tumour cell density over time is equal to the net migration plus the net proliferation of tumour cells. The model uses partial differential equations with two parameters: net rate of migration (D, mm^2/year) and proliferation (ρ, year-1), which can be calculated using routine patient-specific clinical images. This model mimics a virtual *in silico* tumour response to treatment with the same growth kinetics of an individual patient, thus predicting the in vivo treatment response.

In recent years, these mathematical models have been integrated with bio-simulation methods to improve fitting and predictive ability in vivo in terms of treatment-related response. Starting from biomolecular evidence, some authors have developed multiscale models of GBM progression that cover processes from the cellular to the molecular scale. Antipas et al. [67] introduced the oxygen enhancement ratio (OER) in models, and Kim Y. et al. [68] proposed a multiscale mathematical model where cell migration and proliferation are controlled through an intracellular control system via microRNA-451 (miR-451)-AMPK complex in response to glucose availability and physical constraints in the microenvironment. Schuetzet al. [69] also proposed a model integrating the molecular interaction network (miR-451, LKB1 and AMPK) to cellular actions (e.g. chemotactic movement) to explain the regulation of GBM cell migration and proliferation. Swanson et al. [70] tried to integrate tumour-microenvironment interactions of normoxic glioma cells, hypoxic glioma cells, vascular endothelial cells, diffusible angiogenic factors and necrosis formation into a biologically based mathematical PI model for glioma. Specifically for radiotherapy treatment, Holdsworth et al. [71] included the patient-specific description of tumour growth and radiation response in the PI-RT model [64] to generate biologically guided treatment plans. Using an adaptive multi-objective evolutionary algorithm (MOEA), intensity modulated RT (IMRT) plans were optimized using clinical objectives to maximize normal tissue sparing and taking into account the reduction of tumour burden at various time points in order to increase the TCP. Integrative biomolecular mathematical models of kinetics of tumour growth and response to radiotherapy via more complex "biomolecular-integrated" LQ models [72, 73] considering the dynamic instability of radioresistance of GBM (cellular subpopulations, kinetics growth and biomolecular alterations) could support better treatment management of the GBM patients as well as the design of more effective treatment strategies. These speculative investigations of alternative treatment strategies require further investigation before their introduction to clinical practice.

Potential Confounding Factors

The contributions of several potentially confounding factors have not been fully taken into consideration in the currently proposed methods. These factors include: (1) data collection from institutes with different patient selection criteria and different treatment modalities; (2) the possible coexistence of different cell types within the target of enrolled patients, that may explain the variability of parameters and the need for more advanced models; (3) the different expression levels of molecular factors among patients, such as MGMT methylation and (4) other factors, such as hypoxia and reoxygenation that may influence the clinical outcome.

The role of molecular predictors is still under debate and might help in the design of new treatment strategies particularly in older patients with Recursive Partitioning Analysis ≥3. Clinical data have been combined with other predictive factors to improve the recently proposed nomograms [74] with molecular and image-based classifiers.

Finally, the accelerated failure time model has been applied using data from 721 patients with glioblastoma to model factors affecting individualized survival after surgical resection [75]. An increased 2-years survival was associated with age, Karnofsky Performance status, the extension of resection of enhancing tumour on T1-postgadolinium magnetic resonance imaging and adjuvant therapy with external radiotherapy and/or temozolomide.

Conclusion

In conclusion, mathematical models indicate that moderately hypofractionated, high total dose treatment schedules and use of TMZ deserve consideration. Moreover, state-of-the-art modern multimodality imaging techniques permit a better tumour identification and contouring, as well as modern innovative linear accelerator and on-board imaging allow the delivery of high doses to the tumours, sparing the surrounding healthy brain.

References

1. AAPM TG 43. Quality assessment and improvement of dose response models: some effects of study weaknesses on study findings. "C'est Magnifique?" AAPM report 43, 1993
2. Joiner MC, Van der Kogel AJ, Steel GG. Introduction: the significance of radiobiology and radiotherapy for cancer treatment. In: Joiner MC, Van der Kogeleds A, editors. Basic clinical radiobiology. 4th ed. London: Hodder Arnold; 2009.
3. Los M, Rashedi I, Panigrahi S, Klonisch T, Schulze-Osthoff K. Tumor growth and cell proliferation. In: Molls M, Vaupel P, Nieder C, Anschereds MS, editors. The impact of tumor biology on cancer treatment and multidisciplinary strategies. Berlin: Springer; 2009.
4. Willers H, Beck-Bornholdt HP. Origins of radiotherapy and radiobiology: separation of the influence of dose per fraction and overall treatment time on normal tissue damage by Reisner and Miescher in the 1930s. Radiother Oncol. 1996;38:171–3.
5. Bentzen SM. Quantitative clinical radiobiology. Acta Oncol. 1993;32(3):259–75.
6. Strandquist M. A study of the cumulative effects of fractionated X-ray treatment based on the experience gained at radiumhemmet with the treatment of 280 cases of carcinoma of the skin and lip. Acta Radiol. 1944;55(Suppl):300–4.
7. Munro TR, Gilbert CW. The relation between tumour lethal doses and the radiosensitivity of tumour cells. Br J Radiol. 1961;34:246–51.
8. Ellis F. Dose, time and fractionation a clinical hypothesis. Clin Radiol. 1969;20(1):1–7.
9. Walker MD, Strikes TA, Sheline GE. An analysis of dose-effect relationship in the radiotherapy of malignant glioma. Int J Radiat Oncol Biol Phys. 1979;5: 1725–31.
10. Mikhael MA. Radiation necrosis of the brain: correlation between computed tomography, pathology, and dose distribution. J Comput Assist Tomogr. 1978;2(1): 71–80.
11. Fowler JF. The linear quadratic formula and progress in fractionated radiotherapy. Br J Radiol. 1989;62: 679–94.
12. Fowler JF. Sensitivity analysis of parameters in linear-quadratic radiobiologic modeling. Int J Radiat Oncol Biol Phys. 2009;73(5):1532–7.
13. Kellerer AM. Studies of the dose-effect relation. Experientia. 1989;45:13–21.
14. Joiner MC, Bentzen SM. Fractionation: the linear quadratic approach. In: Joiner MC, Van der Kogeleds A, editors. Basic clinical radiobiology. 4th ed. London: Hodder Arnold; 2009.
15. Fowler JF. 21 years of biologically effective dose. Br J Radiol. 2010;83:554–68.
16. Debus J, Abdollahi A. For the next trick: new discoveries in radiobiology applied to glioblastoma. Current concepts and future perspective in radiotherapy of glioblastoma. ASCO education book; 2014. e95–9.
17. Shahine BH, Ng CE, Raaphorst GP. Modelling of continuous low dose rate and accelerated fractionated high dose rate irradiation treatments in a human glioma cell line. Int J Radiat Biol. 1996;70(5): 555–61.
18. Williams JA, Williams JR, Yuan X, Dillehay LE. Protracted exposure radiosensitization of experimental human malignant glioma. Radiat Oncol Investig. 1998;6(6):255–63.
19. Cordes N, Plasswilm L, Sauer R. Interaction of paclitaxel (Taxol) and irradiation. In-vitro differences between tumor and fibroblastic cells. Strahlenther Onkol. 1999;175(4):175–81.
20. Nusser NN, Bartkowiak D, Röttinger EM. The influence of bromodeoxyuridine on the induction and repair of DNA double-strand breaks in glioblastoma cells. Strahlenther Onkol. 2002;178(9):504–9.
21. Garcia LM, Leblanc J, Wilkins D, Raaphorst GP. Fitting the linear-quadratic model to detailed data sets for different dose ranges. Phys Med Biol. 2006;51(11):2813–23.
22. Withers HR, Thames Jr HD, Peters LJ. A new isoeffect curve for change in dose per fraction. Radiother Oncol. 1983;1:187–91.
23. Thames HD, Bentzen SM, Turesson I, Overgaard M, van den Bogaert W. Time-dose factors in radiotherapy: a review of the human data. Radiother Oncol. 1990;19:219–35.
24. Roberts SA, Hendry JH. A realistic closed-form radiobiological model of clinical tumor-control data incorporating intertumor heterogeneity. Int J Radiat Oncol Biol Phys. 1998;41(3):689–99.
25. Joiner MC, Marples B, Lambin P, Short SC, Turesson I. Low-dose hypersensitivity: current status and possible mechanisms. Int J Radiat Oncol Biol Phys. 2001;49(2):379–89.
26. Joiner MC. Quantifying cell killing and cell survival. In: Joiner MC, Van der Kogeleds A, editors. Basic clinical radiobiology. 4th ed. London: HodderArnold; 2009.
27. Haas-Kogan DA, Yount G, Haas M, Levi D, Kogan SS, Hu L, Vidair C, Deen DF, Dewey WC, Israel MA. p53-dependent G1 arrest and p53-independent apoptosis influence the radiobiologic response of glioblastoma. Int J Radiat Oncol Biol Phys. 1996;36(1): 95–103.

28. Williams JR, Zhang Y, Russell J, Koch C, Little JB. Human tumor cells segregate into radiosensitivity groups that associate with ATM and TP53 status. Acta Oncol. 2007;46(5):628–38.
29. Williams JR, Zhang Y, Zhou H, Gridley DS, Koch CJ, Russell J, Slater JS, Little JB. A quantitative overview of radiosensitivity of human tumor cells across histological type and TP53 status. Int J Radiat Biol. 2008;84(4):253–64.
30. Mellor HR, Ferguson DJ, Callaghan R. A model of quiescent tumour microregions for evaluating multicellular resistance to chemotherapeutic drugs. Br J Cancer. 2005;93:302–9.
31. Scopelliti A, Cammareri P, Catalano V, Saladino V, Todaro M, Stassi G. Therapeutic implications of cancer initiating cells. Expert Opin Biol Ther. 2009;9:1005–16.
32. Bao S, Wu Q, McLendon RE, Hao Y, Shi Q, Hjelmeland AB, Dewhirst MW, Bigner DD, Rich JN. Glioma stem cells promote radioresistance by preferential activation of the DNA damage response. Nature. 2006;444:756–60.
33. Zhou W, Sun M, Li GH, Wu YZ, Wang Y, Jin F, Zhang YY, Yang L, Wang DL. Activation of the phosphorylation of ATM contributes to radioresistance of glioma stem cells. Oncol Rep. 2013;30(4):1793–801.
34. Gao X, McDonald JT, Hlatky L, Enderling H. Acute and fractionated irradiation differentially modulate glioma stem cell division kinetics. Cancer Res. 2013;73(5):1481–90.
35. Yu V, Nguyen D, Kupelian P, Kaprealian T, Selch M, Low D, Pajonk F, Sheng K. SU-C-BRE-03: dual compartment mathematical modeling of glioblastoma multiforme (GBM). Med Phys. 2014;41:94.
36. Palumbo S, Pirtoli L, Tini P, Cevenini G, Calderaro F, Toscano M, Miracco C, Comincini S. Different involvement of autophagy in human malignant glioma cell lines undergoing irradiation and temozolomide combined treatments. J Cell Biochem. 2012;113(7):2308–18.
37. Tini P, Palumbo S, Cevenini G., Miracco C., Comincini S., Pirtoli L. Autophagy as potential therapeutical target in glioblastoma. Acts of XXII Italian Congress AIRO. Rome November 17–20th 2012.
38. Palumbo S, Comincini S. Autophagy and ionizing radiation in tumors: the "survive or not survive" dilemma. J Cell Physiol. 2013;228(1):1–8.
39. Tucker SL, Thames HD, Taylor JMG. How well is the probability of tumor cure after fractionated irradiation described by Poisson statistics? Radiat Res. 1990;124:273–82.
40. Webb S, Nahum AE. A model for calculating tumour control probability in radiotherapy including the effects of inhomogeneous distribution of dose and clonogenic cell density. Phys Med Biol. 1993;38:653–66.
41. Niemierko A, Goitein M. Implementation of a model for estimating tumour control probability for an inhomogeneously irradiated tumor. Radiother Oncol. 1993;29:140–7.
42. Okunieff P, Morgan D, Niemierko A, et al. Radiation dose-response of human tumor. Int J Radiat Oncol Biol Phys. 1995;32:1227–37.
43. Verhaak RG, Hoadley KA, Purdom E, Wang V, Qi Y, Wilkerson MD, Miller CR, Ding L, Golub T, Mesirov JP, Alexe G, Lawrence M, O'Kelly M, Tamayo P, Weir BA, Gabriel S, Winckler W, Gupta S, Jakkula L, Feiler HS, Hodgson JG, James CD, Sarkaria JN, Brennan C, Kahn A, Spellman PT, Wilson RK, Speed TP, Gray JW, Meyerson M, Getz G, Perou CM, Hayes DN, Network CGAR. An integrated genomic analysis identifies clinically relevant subtypes of glioblastoma characterized by abnormalities in PDGFRA, IDH1, EGFR and NF1. Cancer Cell. 2010;17(1):98–110.
44. Vlashi E, McBride WH, Pajonk F. Radiation responses of cancer stem cells. J Cell Biochem. 2009;108(2):339–42.
45. Manninoa M, Chalmers AJ. Radioresistance of glioma stem cells: intrinsic characteristic or property of the 'microenvironment-stem cell unit'? Mol Oncol. 2011;5:374–86.
46. Wein LM, Cohen JE, Wu JT. Dynamic optimization of a linear-quadratic model with incomplete repair and volume-dependent sensitivity and repopulation. Int J Radiat Oncol Biol Phys. 2000;47(4):1073–83.
47. Thames Jr HD, Withers HR, Peters LJ, Fletcher GH. Changes in early and late radiation responses with altered dose fractionation: implications for dose-survival relationships. Int J Radiat Oncol Biol Phys. 1982;8(2):219–26.
48. Pedicini P, Fiorentino A, Simeon V, Tini P, Chiumento C, Pirtoli L, Salvatore M, Storto G. Clinical radiobiology of glioblastoma multiforme: estimation of tumor control probability from various radiotherapy fractionation schemes. Strahlenther Onkol. 2014;190(10):925–32. doi:10.1007/s00066-014-0638-9. Epub 2014 Apr 4.
49. Pedicini P. In regard to Pedicini et al. Int J Radiat Oncol Biol Phys. 2013;87(5):858.
50. Bentzen SM. Dose-response relationship in radiotherapy. In: Steel GG, editor. Basic clinical radiobiology. 2nd ed. London: Arnold; 1997. p. 78–86.
51. Salazar OM, Rubin P, Feldstein ML, et al. High dose radiation therapy in the treatment of malignant gliomas: final report. Int J Radiat Oncol Biol Phys. 1979;5:1733–40.
52. Salazar OM, Rubin P, McDonald JV, et al. High dose radiation therapy in the treatment of glioblastoma multiforme: a preliminary report. Int J Radiat Oncol Biol Phys. 1976;1:717–27.
53. Qi XS, Schultz CJ, Li XA. An estimation of radiobiologic parameters from clinical outcomes for radiation treatment planning of brain tumor. Int J Radiat Oncol Biol Phys. 2006;64(5):1570–80.
54. Brenner DJ, Hall EJ. Conditions for the equivalence of continuous to pulsed low dose rate brachytherapy. Int J Radiat Oncol Biol Phys. 1991;20:181–90.
55. Ciammella P, Galeandro M, D'Abbiero N, Podgornii A, Pisanello A, Botti A, Cagni E, Iori M, Iotti C. Hypo-fractionated IMRT for patients with newly

diagnosed glioblastoma multiforme: a 6 year single institutional experience. Clin Neurol Neurosurg. 2013;115(9):1609–14.
56. Pedicini P, Nappi A, Strigari L, Jereczek-Fossa BA, Alterio D, Cremonesi M, Botta F, Vischioni B, Caivano R, Fiorentino A, Improta G, Storto G, Benassi M, Orecchia R, Salvatore M. Correlation between EGFR expression and accelerated proliferation during radiotherapy of head and neck squamous cell carcinoma. Radiat Oncol. 2012;7:143.
57. Pedicini P, Caivano R, Strigari L, Benassi M, Fiorentino A, Fusco V. In regard to Miralbell et al. Re: dose-fractionation sensitivity of prostate cancer deduced from radiotherapy outcomes of 5969 patients in seven international institutional datasets: alpha/beta = 1.4 (0.9–2.2) Gy. Int J Radiat Oncol Biol Phys. 2013;85(1):10–1.
58. Pedicini P, Fiorentino A, Improta G, Nappi A, Salvatore M, Storto G. Estimate of the accelerated proliferation by protein tyrosine phosphatase (PTEN) over expression in postoperative radiotherapy of head and neck squamous cell carcinoma. Clin Transl Oncol. 2013;15(11):919–24.
59. Pedicini P, Strigari L, Benassi M. Estimation of a self-consistent set of radiobiological parameters from hypofractionated versus standard radiation therapy of prostate cancer. Int J Radiat Oncol Biol Phys. 2013;85(5):e231–7.
60. Daşu A, Toma-Daşu I, Fowler JF. Should single distributed parameters be used to explain the steepness of tumour control probability curves? Phys Med Biol. 2003;48:387–97.
61. Swanson KR, Rostomily RC, Alvord EC. A mathematical modelling tool for predicting survival of individual patients following resection of glioblastoma: a proof of principle. Br J Cancer. 2008;98: 113–9.
62. Rockne R, Alvord EC, Rockhill JK, Swanson KR. A mathematical model for brain tumor response to radiation therapy. J Math Biol. 2009;58:561–78.
63. Wang CH, Rockhill JK, Mrugala M, Peacock DL, Lai A, Jusenius K, et al. Prognostic significance of growth kinetics in newly diagnosed glioblastomas revealed by combining serial imaging with a novel biomathematical model. Cancer Res. 2009;69:9133–40.
64. Rockne R, Rockhill JK, Mrugala M, Spence AM, Kalet I, Hendrickson K, Lai A, Cloughesy T, Alvord Jr EC, Swanson KR. Predicting the efficacy of radiotherapy in individual glioblastoma patients in vivo: a mathematical modeling approach. Phys Med Biol. 2010;55(12):3271–85.
65. Roniotis A, Marias K, Sakkalis V, Manikis GC, Zervakis M. Simulating radiotherapy effect in high-grade glioma by using diffusive modeling and brain atlases. J Biomed Biotechnol. 2012;2012:715812.
66. Tracqui P, Cruywagen GC, Woodward DE, Bartoo GT, Murray JD, Alvord Jr EC. A mathematical model of glioma growth: the effect of chemotherapy on spatio-temporal growth. Cell Prolif. 1995;28(1):17–31.
67. Antipas VP, Stamatakos GS, Uzunoglu NK, Dionysiou DD, Dale RG. A spatio-temporal simulation model of the response of solid tumours to radiotherapy in vivo: parametric validation concerning oxygen enhancement ratio and cell cycle duration. Phys Med Biol. 2004;49(8):1485–504.
68. Kim Y. Regulation of cell proliferation and migration in glioblastoma: new therapeutic approach. Front Oncol. 2013;3:53.
69. Schuetz TA, Becker S, Mang A, Toma A, Buzug TM. A computational multiscale model of glioblastoma growth: regulation of cell migration and proliferation via microRNA-451, LKB1 and AMPK. Conf Proc IEEE Eng Med Biol Soc. 2012;2012:6620–3.
70. Swanson KR, Rockne RC, Claridge J, Chaplain MA, Alvord Jr EC, Anderson AR. Quantifying the role of angiogenesis in malignant progression of gliomas: in silico modeling integrates imaging and histology. Cancer Res. 2011;71(24):7366–75.
71. Holdsworth CH, Corwin D, Stewart RD, Rockne R, Trister AD, Swanson KR, Phillips M. Adaptive IMRT using a multiobjective evolutionary algorithm integrated with a diffusion-invasion model of glioblastoma. Phys Med Biol. 2012;57(24):8271–83. doi:10.1088/0031-9155/57/24/8271. Epub 2012 Nov 29.
72. Leder K, Pitter K, Laplant Q, Hambardzumyan D, Ross BD, Chan TA, Holland EC, Michor F. Mathematical modeling of PDGF-driven glioblastoma reveals optimized radiation dosing schedules. Cell. 2014;156(3):603–16.
73. Jamali Nazari A, Sardari D, Vali AR, Maghooli K. Computer implementation of a new therapeutic model for GBM tumor. Comput Math Methods Med. 2014;2014:481935. Epub 2014 Aug 5.
74. Gorlia T, van den Bent MJ, Hegi ME, Mirimanoff RO, Weller M, Cairncross JG, Eisenhauer E, Belanger K, Brandes AA, Allgeier A, Lacombe D, Stupp R. Nomograms for predicting survival of patients with newly diagnosed glioblastoma: prognostic factor analysis of EORTC and NCIC trial 26981-22981/CE.3. Lancet Oncol. 2008;9(1):29–38. Epub 2007 Dec 21.
75. Marko NF, Weil RJ, Schroeder JL, Lang FF, Suki D, Sawaya RE. Extent of resection of glioblastoma revisited: personalized survival modeling facilitates more accurate survival prediction and supports a maximum-safe-resection approach to surgery. J Clin Oncol. 2014;32(8):774–82. doi:10.1200/JCO.2013.51.8886. Epub 2014 Feb 10.